The Japan Society of Mechanical Engineers

X-Ray Study of Mechanical Properties of TiN Thin Films Coated on Steel by Ion Beam Mixing Method*

Toshimasa ITO**, Keisuke TANAKA***,
Yoshiaki AKINIWA***, Takahiro ISHII**
and Yasuhiro MIKI****

The thin films of titanium nitride (TiN) with the thickness of 0.5, 1.0, 2.0, 4.0 μm were coated on a steel substrate by the ion beam mixing method. The film had a strong fiber texture with <110> axis perpendicular to the film surface. The initial residual stress was equi-biaxial compression between −4.4 to −5.6 GPa. For all thickness cases, the initial part of the changes of the in-plane stresses in the film due to external tensile loading agreed well with the prediction based on elasticity. While the substrate was under an uniaxial stress, the film was in the biaxial state of stress because of the mismatch of Poisson's ratio. When the measured stress in the film exceeded a certain value, the stress departed from the linear relation and leveled off. The onset of nonlinearity was nearly coincident with the first appearance of cracks. The stresses at the onset of nonlinearity and leveling-off decreased with increasing film thickness. The ratio of Young's modulus between loading and unloading decreased as the film thickness increased.

Key Words: X-ray Stress Analysis, TiN Film, Reuss Model, Residual Stress, Loading Stress, Four-point Bending, Stress-strain Curve, Fracture Strength

1. Introduction

Hard film coating has been widely used to increase the wear resistance and heat resistance of machine parts. Among various methods of coating, the ion beam mixing (IBM) method has excellent adhesion properties, because the mixing layer is formed between film and substrate. In the IBM method, the texture of coated films can be controlled to have the fiber texture of <001>, <110> or <111> perpendicular to the film surface[1]. The mechanical properties of films depend on the residual stress in the film as well as on the texture and microstructure. The fracture strength of films will be determined by the sum of the residual and externally applied stresses. In order to measure the stress, the X-ray diffraction method has been used. The present authors proposed a new X-ray method to measure the stress in the film with fiber textures in their previous papers[2],[3].

In the present paper, the X-ray method was used to measure the stress in TiN thin films deposited on a steel substrate by the IBM method. TiN thin films had a fiber texture with fiber axis of <110> direction perpendicular to the film surface. Four-point bending was applied to coated specimens, and the stresses in the film and substrate were simultaneously measured by the X-ray method. The microstructural feature of the film surface was examined by scanning electron microscopy (SEM).

2. Experimental Procedure

2.1 Material and specimen

The substrate was a medium-carbon steel with a carbon content of 0.45% (JIS S45C) and had the dimensions of 10 mm in width, 50 mm in length and 4 mm in thickness. The substrate specimen was

* Received 14th February, 2002 (No. 02-4025)
** Graduate School, Nagoya University, Chikusa-ku, Nagoya 464-8603, Japan. E-mail: toshi_i@mbox.media.nagoya-u.ac.jp
*** Department of Mechanical Engineering, Nagoya University, Chikusa-ku, Nagoya 464-8603, Japan
**** Nara Prefectural Institute of Industrial Technology, Kashiwagi-cho, Nara 630-8031, Japan

NII-Electronic Library Service

The Japan Society of Mechanical Engineers

annealed at 850°C for 1 h after polished, and then finished by buffing with 0.05 μm alumina powder. The TiN film was deposited in an ion beam mixing equipment (Hitachi IMX-40-20-W). Table 1 shows the deposition conditions of thin films. In the coating process, the specimens were first subjected to the nitrogen ion injection process, and then to the IBM process. In both processes, the acceleration voltage was 20 kV and the nitrogen ion electric current density was 2.0 A/m². The thickness of the coated films was 0.5, 1.0, 2.0 and 4.0 μm. Figure 1 shows the diffraction profiles of the films with various thicknesses taken by the Cr-Kα radiation under the X-ray conditions described in the next section. The peak of 220 diffraction is very strong and a small peak of 200 diffraction is also seen. The film has a strong fiber texture with the axis <110> perpendicular to the film surface. The peaks of 110, 200 and 211 diffractions from the steel substrate are observed and the intensity of 211 diffraction is strong enough to measure the stress even for the case of the thickness of 4.0 μm.

2.2 X-ray stress measurement

Under four-point bending, the stresses in thin film and steel substrate were measured simultaneously on the tensile surface in two directions, the loading direction, σ_{11}, (the longitudinal direction) and the direction perpendicular to it, σ_{22}, (the transverse direction), as shown in Fig. 2. In the figure, E and ν are Young's modulus and Poisson's ratio of the film, and E_s and ν_s are those for the substrate. A strain gage was glued on the coated surface of the specimen to monitor the applied strain.

The X-ray equipment with a rotating anode (Mac Science, MXP18, MX21) was used for stress measurement. The diffractometer has parallel beam optics and the side-inclination method (Ω-goniometer) was adapted. Table 2 summarizes the X-ray conditions. The diffraction of TiN 220 by Cr-Kα was used to measure the stress. The diffraction angle of strain free samples was $2\theta_0=99.66$ deg. The diffraction angle was measured at two inclination angles, 0 and 60 deg, because of the fiber texture of the thin film[2),(3)].

For the <110> fiber textured film, the stress state in TiN film is assumed to be plane stress, i.e. $\sigma_{33}=\sigma_{23}=\sigma_{31}=0$, and also $\sigma_{12}=0$. The nonzero stress components are the longitudinal stress along the loading axis, σ_{11}, and the transverse stress perpendicular to the loading axis, σ_{22} on the specimen surface as shown in Fig. 2. As reported in our previous papers[2),(3)], Reuss model[4)] gives the following linear relation between the X-ray measured strain and stress in films:

$$\frac{(\varepsilon_{\phi=0^\circ}+\varepsilon_{\phi=90^\circ})}{2}=\left(\frac{S_0}{8}\overline{\cos 2\beta}+\frac{S_0+2S_{44}}{8}\right)(\sigma_{11}+\sigma_{22})\sin^2\psi+\frac{S_0+4S_{12}}{4}(\sigma_{11}+\sigma_{22}) \quad (1)$$

$$\frac{(\varepsilon_{\phi=0^\circ}-\varepsilon_{\phi=90^\circ})}{2}=\left[\left(\frac{3S_0+4S_{44}}{16}+\frac{3S_0}{16}\overline{\cos 4\beta}\right.\right.$$

Table 1 Coating conditions of TiN films

Nitrogen ion injection process	Acceleration voltage (kV)	20			
	Nitrogen ion electric current density (A/m²)	2.0			
	Process time (min)	13.3			
	Dose rate (ions/m²)	1.0×10^{22}			
	Vacuum container pressure (Pa)	7.3×10^{-3}~8.0×10^{-3}			
IBM process	Acceleration voltage (kV)	20			
	Nitrogen ion electric current density (A/m²)	2.0			
	Deposition speed (nm/s)	0.75			
	Process time (min)	13.9	27.8	55.6	111.2
	Vacuum container pressure (Pa)	1.2×10^{-4}~8.0×10^{-4}			
	Thickness (μm)	0.5	1.0	2.0	4.0
	Specimen temperature (°C)	361			

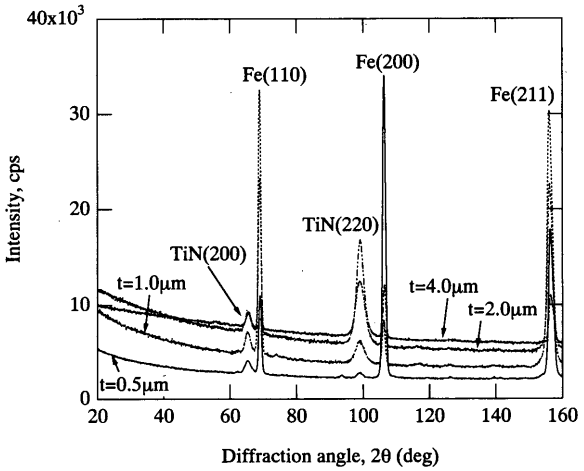

Fig. 1 X-Ray diffraction profiles of the film

Table 2 X-ray measurement conditions

Material	TiN film thickness (μm)			S45C
	4	2, 1	0.5	
Characteristic X-rays	Cr-Kα			
Diffraction plane	220			211
Diffraction angle (deg)	99.66			156.41
Tilt angle $\sin^2\psi$	0, 0.75			0~0.6
Tube voltage (kV)	40	30		
Tube current (mA)	200	200		
Scanning speed (deg/s)	3/4	1	1/2	1
Preset time (s)	3	2	4	2

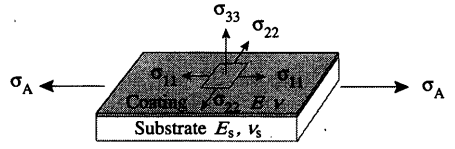

Fig. 2 Coated thin film under uniaxial tension

NII-Electronic Library Service

The Japan Society of Mechanical Engineers

$$+\frac{3s_0}{8}\overline{\cos 2\beta}\Big)\sin^2\psi-\frac{s_0}{4}\overline{\cos 2\beta}\Big](\sigma_{11}-\sigma_{22}) \quad (2)$$

where $\varepsilon_{\phi=0}$ is the X-ray measured strain in the longitudinal direction, $\varepsilon_{\phi=90}$ is the transverse direction, s_{ij} is the elastic compliance of single crystals, and β is the orientation angle of a crystal[2),3)]. The elastic compliances of single crystals of TiN[5)] are presented in Table 3. The table also shows the mechanical Young's modulus and Poisson's ratio of <110> fiber textured film calculated by Reuss model[3)]. The mean values of $\overline{\cos 2\beta}$ and $\overline{\cos 4\beta}$ depend on the diffraction plane and inclination angle. In this study, $\overline{\cos 2\beta}$ and $\overline{\cos 4\beta}$ are 0 for $\psi=0$ deg, and 0.333 3 and $-0.777\,8$ for $\psi=60$ deg. The details of this method is reported in our previous papers[2),3)]. By using Eqs. (1) and (2), the stress components σ_{11} and σ_{22} can be determined from the measured values of $\varepsilon_{\phi=0}$ and $\varepsilon_{\phi=90}$ at $\psi=0$ and 60 deg. Since there is not much difference in the stress values determined by Reuss and Voigt models[2),3),6)], the stress values determined by Reuss model are presented in the present report.

The stress in the steel substrate was measured from the Fe 211 diffraction obtained by irradiating Cr-Kα radiation through the thin film. The diffraction angle was $2\theta_0=156.4$ deg. The $\sin^2\psi$ method was used for stress calculation and the stress constant was -318 MPa/deg[7)].

2.3 Microscopic observation

The surface of the specimen with the film thicknesses of 0.5 and 4.0 μm was replicated with cellulose acetate sheets when the stress measurement was conducted at various applied strains. The replica was examined by SEM (JEOL JSM-6330F) after gold coating at a acceleration voltage of 5 kV. For the other specimens, SEM observation was conducted only before loading and after unloading. The direct SEM observation of the specimen surface was conducted at a acceleration voltage of 5 kV without gold coating.

3. Experiment Results and Discussion

3.1 Residual and loading stresses in thin film

The changes of the stresses in the loading direction, σ_{11}, and in the perpendicular direction, σ_{22}, in the TiN film with the applied strain ε_A are shown in Fig. 3, where (a), (b), (c) and (d) are for the cases of the thickness of 0.5, 1.0, 2.0 and 4.0 μm, respectively. The bending strain was applied stepwise upto about 15 to 20×10^{-3} and then unloaded. In all cases, the initial residual stresses are equi-biaxial compression, and they are -5.0, -5.6, -4.4 and -5.5 GPa for the cases of the thickness of 0.5, 1.0, 2.0 and 4.0 μm respectively.

For all cases, as the applied strain increases, the stress σ_{11} increases linearly from the compression and then begins to show a nonlinearity followed by leveling. The stress in the perpendicular direction, σ_{22}, decreases with the applied strain. The rate of decrease starts to increase nearly at the same time when the stress σ_{11} deviates from the linearity.

According to SEM observations, the onset of nonlinearity was coincident with the start of cracking. The arrows shown in (a) and (d) indicate the point of first observation of cracking as described later. The stresses at the onset of nonlinearity are 0, -800, $-1\,200$ and $-1\,800$ MPa for the case of the film thickness of 0.5, 1.0, 2.0 and 4.0 μm, respectively. Cracking starts at the lower stress in the thicker films. The stress value at leveling decreases with increasing film thickness. They are about 800, 0, -500 and $-1\,000$ MPa for the cases of 0.5, 1.0, 2.0 and 4.0 μm in thickness, respectively. The reason of decreasing fracture strength for thicker films is not yet clear. The distribution of the residual stress may have the influence of the measured fracture strength. This line of study is now being undertaken.

Table 4 shows the ratio of Young's modulus between loading and unloading. The ratio decreases with increasing thickness, which suggests the increasing cracked area.

3.2 Residual and loading stresses in substrate

The changes of the stresses in the longitudinal direction, σ_{11}, and in the transverse direction, σ_{22}, in the steel substrate with the applied strain ε_A are shown in Fig. 4, where (a), (b), (c) and (d) are the cases of the film thicknesses of 0.5, 1.0, 2.0 and 4.0 μm, respectively. Figure 5 shows the relation between the stress and applied strain obtained for the steel substrate without coating. In all cases of coating, the initial residual stress in the substrate was equi-biaxial compression.

During loading, the longitudinal stress increases linearly with the applied strain. For the cases of thickness 0.5, 1.0 and 2.0 μm, yielding starts at about

Table 3 Elastic constants of single crystal and TiN films

Single crystal elastic compliance				Meachanical elastic constans Film with <110> texture	
				Reuss model	
s_{11} (1/TPa)	s_{12} (1/TPa)	s_{44} (1/TPa)	s_0 (1/TPa)	Young's modulus E (GPa)	Poisson's ratio ν
2.170	-0.380	5.950	-0.425	424	0.195

Table 4 Apparent Young's modulus ratio between loading and unloading

Film thickness	0.5	1.0	2.0	4.0
Apparent Young's ratio E_{unload}/E_{load}	0.81	0.74	0.59	0.19

NII-Electronic Library Service

The Japan Society of Mechanical Engineers

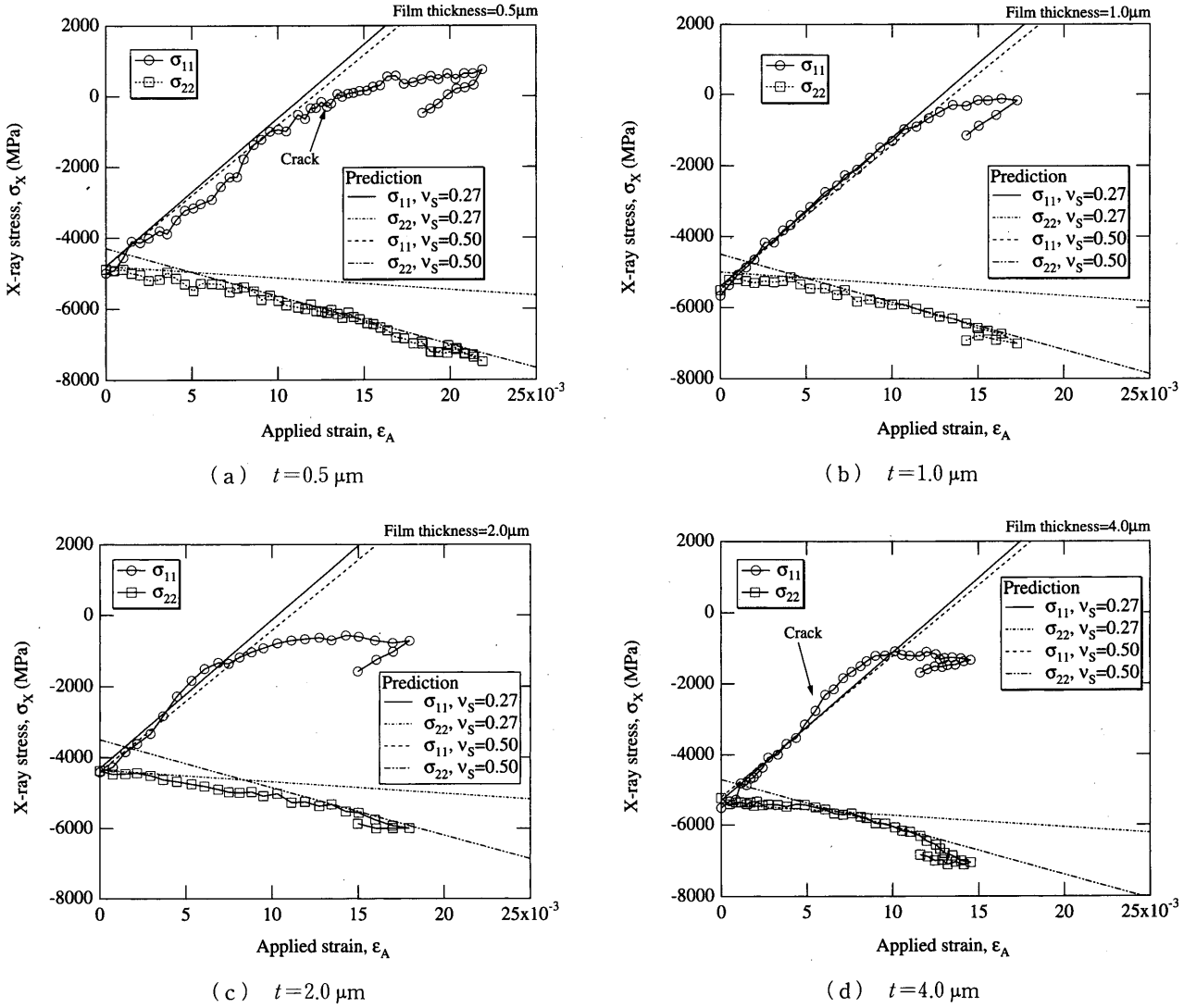

Fig. 3 Change of stress in TiN film due to applied strain

300 MPa, and plastic flow continues under about 500 MPa. The flow stress of 500 MPa in coated substrate is slightly higher than the stress of 350 MPa for non-coated specimens. This increase is caused by peening of N and Ti atoms into the substrate. The change of the stress during unloading is again elastic. For the case of $t=4.0$ μm, the yield starts at 400 MPa and then drops down to 200 MPa. This may be caused by softening due to long time heating in the coating process. The deposition temperature measured on the back of the substrate was 361°C as shown in Table 1. The temperature on the coating surface was expected to be high enough to cause softening.

The transverse stress does not change during initial elastic deformation, and the steel substrate is subjected to a uniaxial stress. The yielding relaxes the transverse compressive stress.

3.3 Prediction of loading stresses in thin films

Under four-point bending, the applied stress in the substrate is uniaxial as shown in Fig. 2. The stress in the film can be calculated when the uniaxial stress is applied to the substrate. Since the film sticks to the substrate, the in-plane strains in the film, ε_{11} and ε_{22}, are equal to those in the substrate. The stress state in the thin film is the plane stress state, and the stresses due to the applied strain ε_A in the film are expressed by

$$\sigma_{11}=\frac{E}{1-\nu^2}(\varepsilon_{11}+\nu\varepsilon_{22})=\frac{1-\nu\nu_s}{1-\nu^2}E\varepsilon_A \quad (3)$$

$$\sigma_{22}=\frac{E}{1-\nu^2}(\varepsilon_{22}+\nu\varepsilon_{11})=\frac{\nu-\nu_s}{1-\nu^2}E\varepsilon_A \quad (4)$$

where ε_A is the applied strain. The measure stress is the sum of the above applied stress and the residual stress. The stress state in the film is biaxial state even under uniaxial loading because of the mismatch of Poisson's ratio.

The slopes of the above relations between the stress and ε_A are drawn in Fig. 3, where Poisson's ratio of the substrate is assumed to be 0.27 for elastic deformation and 0.5 for plastic deformation. The mechanical values of Young's modulus and Poisson's

NII-Electronic Library Service

The Japan Society of Mechanical Engineers

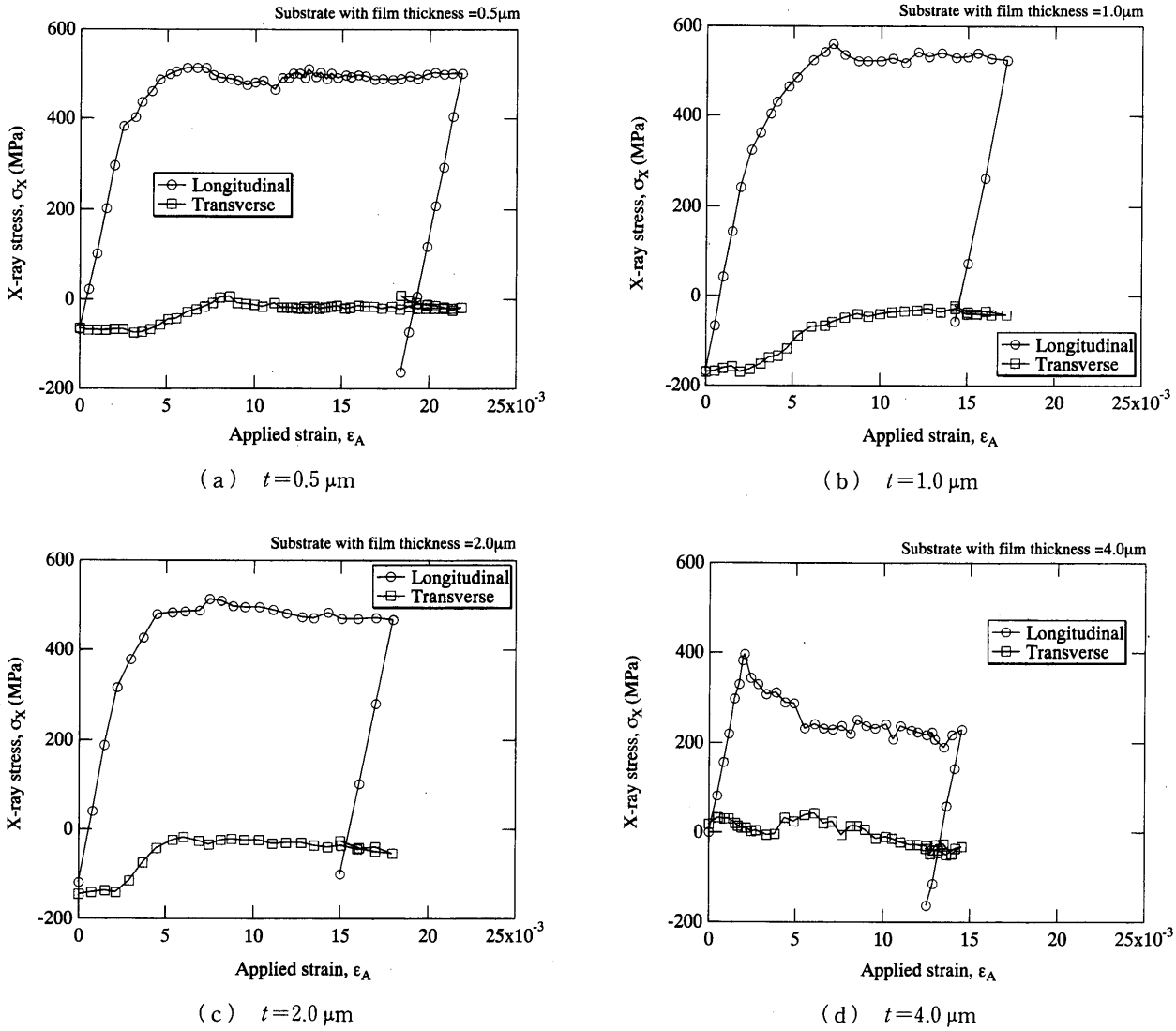

(a) $t=0.5\ \mu m$ (b) $t=1.0\ \mu m$

(c) $t=2.0\ \mu m$ (d) $t=4.0\ \mu m$

Fig. 4 Change of stress in steel substrate due to applied strain

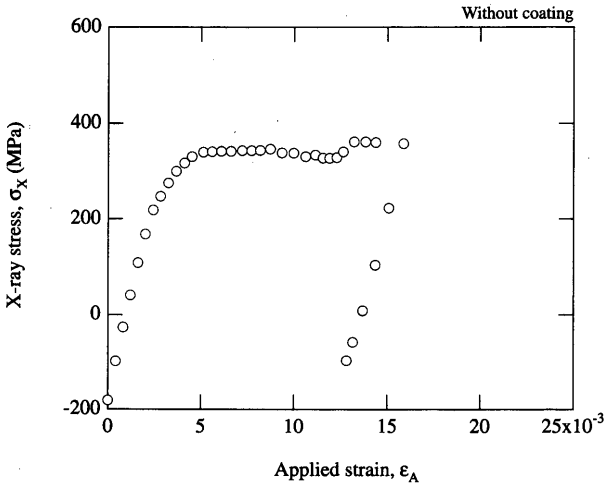

Fig. 5 Change of stress in steel substrate without coating due to applied strain

ratio of the films are presented in Table 3. The initial part of the stress change in the film follows the line of $\nu_s=0.27$, and then follows the line of $\nu_s=0.5$. During unloading, the slope of the measured stress with the strain again follows the relation predicted by using $\nu_s=0.27$ as clearly seen in the data of the transverse stress.

3.4 Microscopic observation

SEM micrographs taken from the replica of the specimen surface with the film thickness 0.5 μm are shown in Fig. 6, where the loading axis is horizontal. No crack is seen at $\varepsilon_A=14.0\times10^{-3}$ and a vertical crack is observed at $\varepsilon_A=14.7\times10^{-3}$. At $\varepsilon_A=19.3\times10^{-3}$, several other cracks can be detected. The strain $\varepsilon_A=14.7\times10^{-3}$ is indicated with the arrow in Fig. 3 (a), and is nearly identical to the point of the departure from the linear relation between stress and strain. Similar results were obtained for the case of the film thickness 4.0 μm.

NII-Electronic Library Service

The Japan Society of Mechanical Engineers

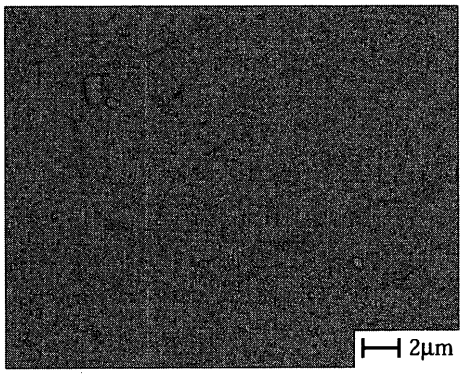

(a) $\varepsilon_A=14.0\times10^{-3}$

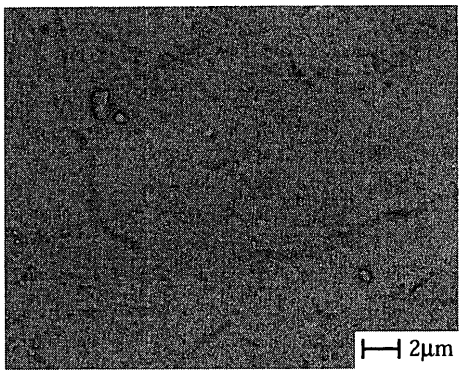

(b) $\varepsilon_A=14.7\times10^{-3}$

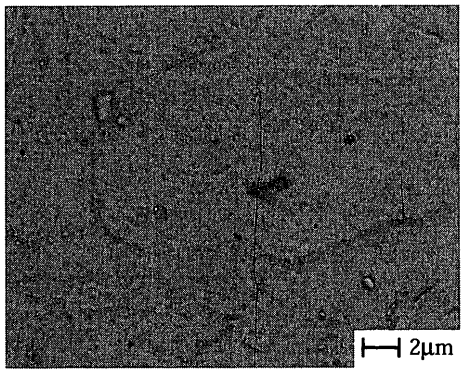

(c) $\varepsilon_A=19.3\times10^{-3}$

Fig. 6 SEM micrographs of the replica of the film surface of the specimen subjected to tensile strain (thickness: $t=0.5$ μm)

Figure 7 shows SEM micrographs taken directly from the unloaded specimen. In all cases, cracks can be observed, and the density of cracks tends to decrease with increasing thickness. The grain size of TiN is much less than one micrometer. The crack path is either transcrystalline or intercrystalline. The opening of cracks are observed in the unloaded specimens even when the X-ray stress is compression. The distribution of the residual stress will play an important role in cracking and will be studied in the future.

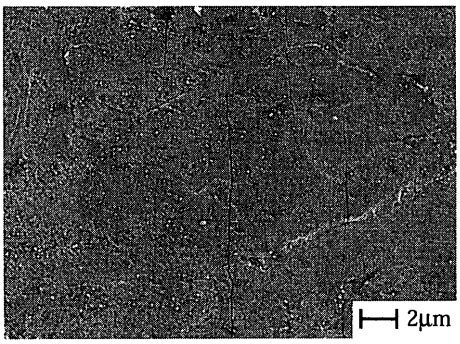

(a) $t=0.5$ μm

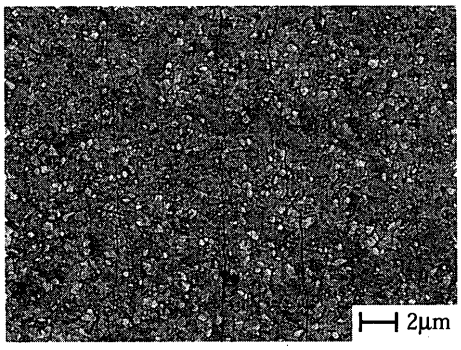

(b) $t=1.0$ μm

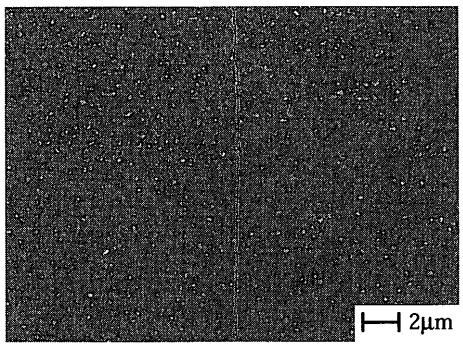

(c) $t=2.0$ μm

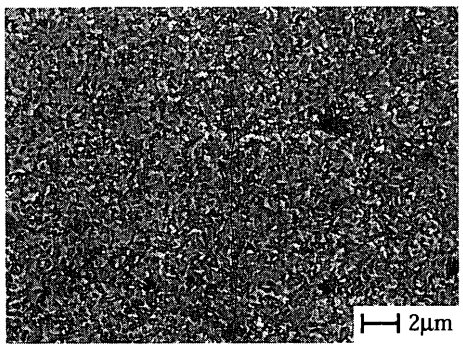

(d) $t=4.0$ μm

Fig. 7 SEM micrographs of the surface of the after unloading specimens

4. Conclusions

The X-ray method is used to measure the stress in polycrystalline TiN thin films having fiber texture

NII-Electronic Library Service

The Japan Society of Mechanical Engineers

with the axis of <110> perpendicular to the film surface. The results are summarized at follows:

(1) The film had a strong fiber texture with <110> axis perpendicular to the film surface. The initial residual stresses were equi-biaxial compression and they were −5.0, −5.6, −4.4 and −5.5 GPa for the cases of the thickness of 0.5, 1.0, 2.0 and 4.0 μm, respectively.

(2) For all thickness cases, the initial part of the changes of the in-plane stresses in the film due to external tensile loading agreed well with the prediction based on elasticity. While the substrate was under an uniaxial stress, the film was in the biaxial state of stress because of the mismatch of Poisson's ratio.

(3) When the measured stress in the film exceeded a certain value, the stress departed from the linear relation and leveled off even though the applied strain keep increasing. The onset of nonlinearity was coincident with the first appearance of cracks and the leveling of the stress was caused by cracking of the film.

(4) The stresses at the onset of nonlinearity and leveling-off decreased with increasing film thickness. The thicker films had the lower fracture strength.

(5) The ratio of Young's modulus between loading and unloading decreased as the film thickness increased, suggesting the increasing cracked area.

References

(1) Miki, M., Araki, H., Taniguchi, T., Nishibata, Y. and Yakushiji, M., J. Soc. Mater., Japan, Vol. 46 (1997), pp. 933-938.

(2) Tanaka, K., Akiniwa, Y., Ito, T. and Inoue, K., JSME Int. J. Ser. A, Vol. 42, No. 2 (1999), pp. 224-234.

(3) Tanaka, K., Ito, T., Akiniwa, Y., Kimachi, H. and Miki, Y., Mater. Sci. Res. Inter., Vol. 6, No. 4 (2000), pp. 231-236.

(4) Reuss, A., Z. Angew. Math. Mech., Vol. 9 (1929), p. 49.

(5) Perry, A.J., Thin Solid Films, Vol. 170 (1989), pp. 63-70.

(6) Voigt, W., Lehrbuch der Kristallphysik, Teubner, (1928), p. 962, Berlin and Leipzig.

(7) Standard Method of X-ray Stress Measurement, (in Japanese), (1997), The Society of Materials Science, Japan.

NII-Electronic Library Service